Electronic Supplementary Information (ESI)

3D interconnected SnO_2-coated Cu foam as a high-performance anode for lithium-ion battery applications

Ji Hyun Um, Hyeji Park, Yong-Hun Cho, Matthew P. B. Glazer, David C. Dunand, Heeman Choe, and Yung-Eun Sung**

1. Materials synthesis

A tin oxide-based sol was prepared by dissolving 0.338 g of $SnCl_2 \cdot 2H_2O$ in a solvent mixture consisting of 0.03 mL 37% hydrochloric acid and 0.47 mL ethanol to obtain a 3 M Sn(II) solution,[S1,S2] which was subsequently aged at room temperature for 24 h. Triple deionized water (DI-H_2O) was then added to the solution, which was aged for another 24 h. Commercially available Cu foam (purchased from Korea Metalfoam company) was punched 11 mm in diameter to fit electrode size and immersed in the prepared gel for 24 h. Solvent evaporation was then conducted at 80 °C in vacuum. A heat treatment was carried out at 500 °C under Ar atmosphere for 2 h to convert the tin oxide precursor gel into crystalline SnO_2 and to obtain final product as an electrode (Fig. S1, ESI†). For the comparison of sol-gel concentration effect on electrochemical performance, the SnO_2-coated Cu foam (SnO_2/Cu foam) from a 10 M Sn(II) solution was prepared by the same experimental procedure (1.128 g of $SnCl_2 \cdot 2H_2O$ in a solvent mixture consisting of 0.03 mL 37% hydrochloric acid and 0.47 mL ethanol as a 10 M Sn(II) solution). SnO_2/Cu foams from 3 M and 10 M were referred to as SnO_2/Cu foam@3M and SnO_2/Cu foam@10M, respectively, and electrochemically tested.

2. Electrochemical measurement

The SnO_2/Cu foam was directly used as a working electrode and assembled into a coin cell without the addition of any binding or conductive materials, and was compared with a SnO_2 powder electrode (SnO_2 NPs) as control. Commercial SnO_2 powder (<100 nm, purchased from Aldrich) was mixed with Ketchen Black as a conductive agent and PVDF in N-methyl-2-pyrrolidone solvent as a binder. The SnO_2 powder : Ketchen Black : PVDF weight ratio was 80:10:10. The mixed slurry was uniformly plated onto Cu foil as a current collector by using a doctor blade method. The electrode was dried under vacuum at 120 °C for 8 h and was then pressed at room temperature. A 2032-type coin cell, consisting of the SnO_2/Cu foam as the working electrode, lithium metal as both the counter and reference electrodes, and a polypropylene separator, was assembled in a glove box under dry Ar atmosphere. The electrolyte used in this study was 1.0 M $LiPF_6$ dissolved in a mixture of ethylene carbonate (EC) and diethyl carbonate (DEC) in a volume ratio of 1 : 1. A galvanostatic test (WBCS3000 cycler, WonA Tech, Korea) was carried out on the coin cell.

3. Characterization

XRD patterns were obtained on a Bruker D-5005 with Cu Kα radiation (λ = 1.5406 Å) operating at 40 kV and 40 mA with a scan range of 20–80°. The morphologies of specimens were characterized by carrying out field emission scanning electron microscopy (FE-SEM, Hitachi S-4800). FE-SEM images using focused ion beam (FIB) milling were taken with Carl Zeiss SUPRA 55VP and Carl Zeiss AURIGA.

In Operando X-ray diffraction measurements were performed at the Advanced Photon Source (Argonne National Laboratory, IL, USA), at the beam-line station 17-BM. A monochromatic X-ray beam approximately 300 μm in diameter at an energy of 17.00 keV (λ

= 0.07291 nm) was transmitted through the thickness of a type 2032 coin cell containing the SnO_2/Cu foam (components as described previously). A 3mm hole was punched through each casing face, covered with a Kapton film (DuPont, DE USA) and sealed with Torr Seal (Kurt J. Lesker Company, PA, USA) to create an X-ray window for characterization. One diffraction pattern was collected every 10 minutes, and each pattern was recorded during collection with a 30 s exposure time onto an a-Si PerkinElmer 2048 x 2048 pixel area detector with a 200 x 200 μm pixel size and a 16-bit dynamic range placed at approximately 250 mm from the sample. A powder sample of LaB6 (NIST SRM-660b) was used as a reference to determine the geometry of the instrument, experimental setup, and sample to detector distance. The electrochemical cell was first cycled at C/3 for two cycles, followed by a rate of 1C for 26 cycles. The Cu (111) fine-grained and uniform diffraction ring from the Cu foam scaffold was fit to a pseudo-Voight function to determine the lattice strains induced in the scaffold by the volume expansion/contraction of the SnO_2 coating layer during electrochemical cycling. Calibration parameters, such as sample-to-detector distance and beam center, were determined using FIT2D[S5,S6] from the LaB6 diffraction pattern collected under the same conditions as the in operando cycling. Lattice strains from the Cu (111) diffraction rings were determined using methods and a series of MATLAB programs developed at the Advanced Photon Source[S7]. The Cu (111) diffraction ring over the area detector was divided into 10° azimuthal slices and fit independently in each slice. The pseudo-Voight shape fitting parameters for 35 out of 36 possible sections were averaged to describe the average observed d-spacing of the peak under examination (one section was omitted due to the beam-stop shadow on the detector). The average observed crystallographic strain was calculated using the following equation:

$$\varepsilon_{Cu(111)} = \frac{d_{(111)} - d^{0}_{(111)}}{d^{0}_{(111)}}$$

where d^0 refers to the first diffraction pattern collected during the experiment, as the initial strain-free d^0 is unknown. In order to demonstrate the repeatability of the cyclic strain behavior and to partially correct for instrumental drift which occurred during the experiment, the strain curves in Fig. S8 for cycles 5, 10 and 15 were offset by strains of -1, 1.5 and -4 X 10^{-5} respectively.

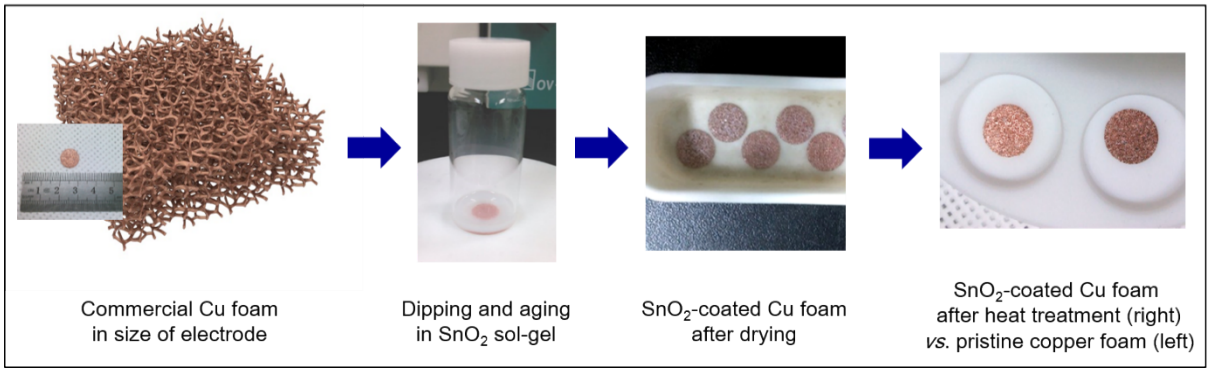

Fig. S1 Fabrication process of SnO_2/Cu foam electrode through a sol-gel method.

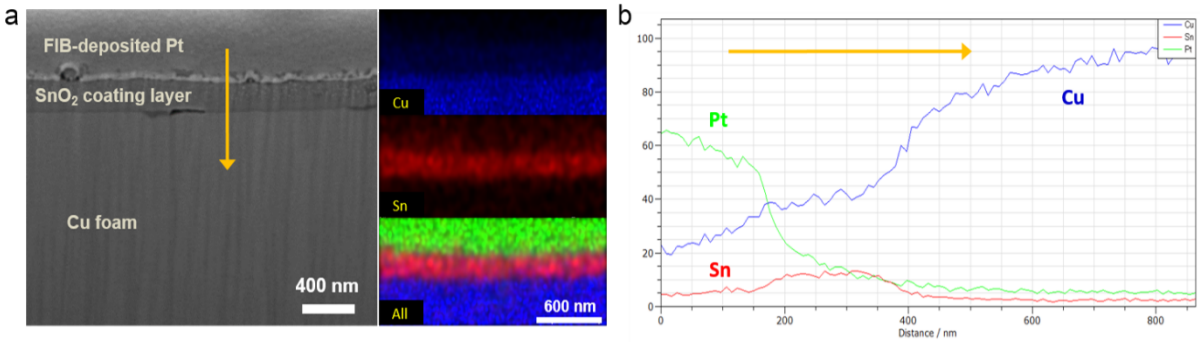

Fig. S2 (a) SEM and EDX mapping images of SnO_2/Cu foam after FIB milling and (b) EDX line scan result across the SnO_2 coating layer as indicated by the arrow dire ction.

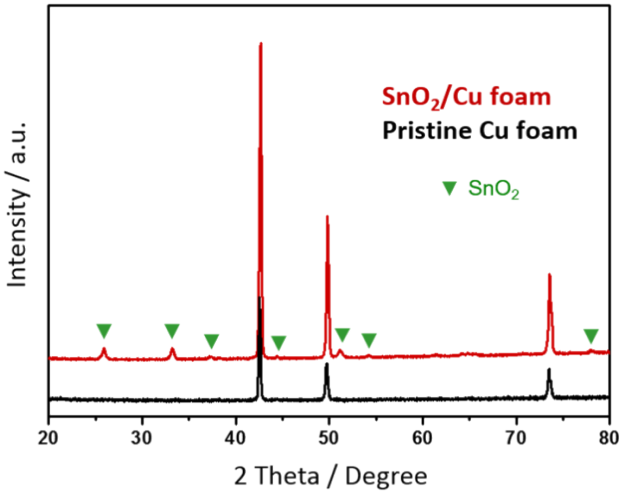

Fig. S3 XRD patterns of pristine Cu foam and SnO_2/Cu foam after heat treatment at 500 under Ar atmosphere.

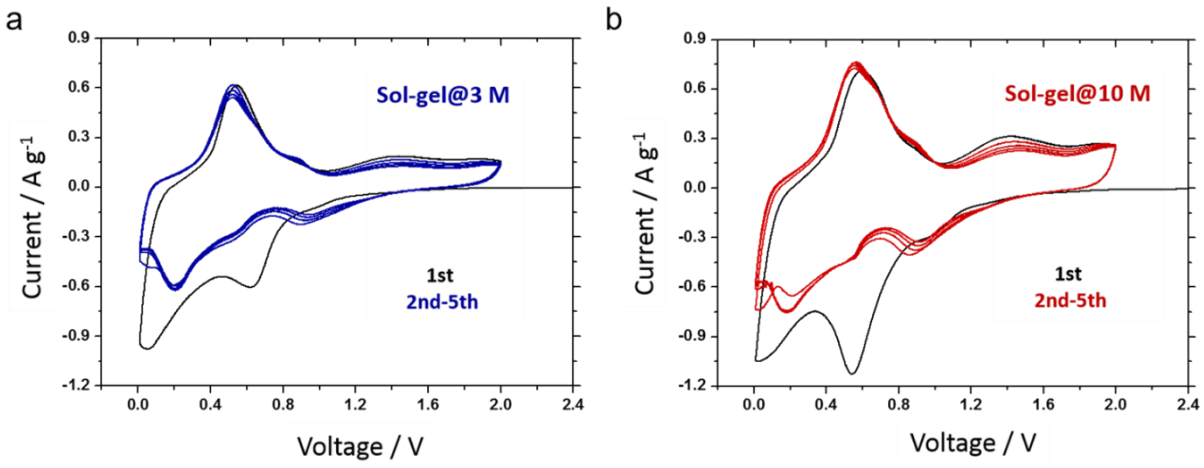

Fig. S4 Cyclic voltammograms of (a) SnO_2/Cu foam@3M and (b) SnO_2/Cu foam@10M at the first five cycles at a scan rate of 0.1 mV s^{-1} between 0.01 V and 2 V.

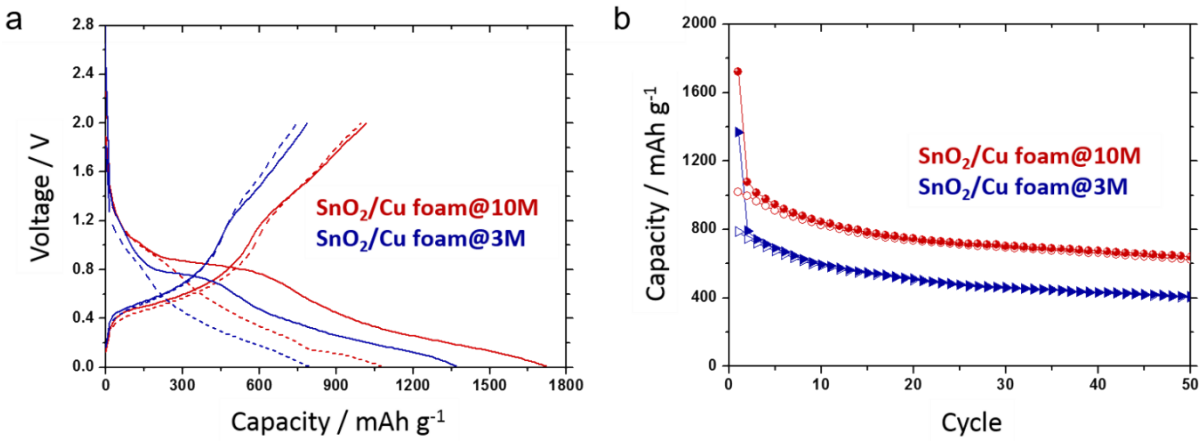

Fig. S5 (a) Discharge/charge curves of SnO_2/Cu foam@3M and SnO_2/Cu foam@10M at the 1st (solid line) and 2nd (dash line) cycles at 1 C and (b) capacity comparison of SnO_2/Cu foam@3M and SnO_2/Cu foam@10M at 1 C.

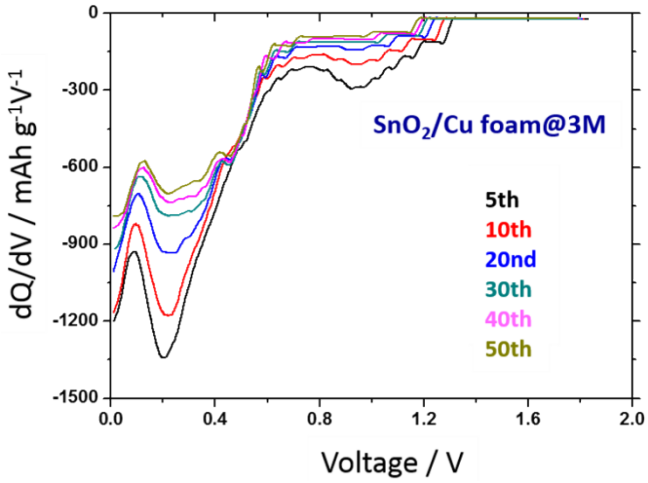

Fig. S6 dQ/dV profiles of SnO_2/Cu foam@3M at selected cycles at 1 C.

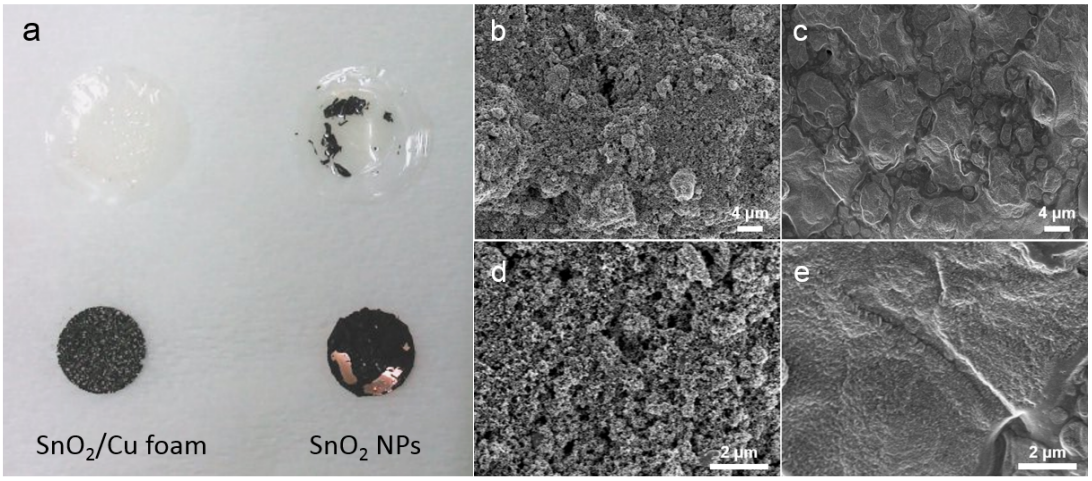

Fig. S7 (a) Phtograph of disassembled electrodes and separators, SEM images of disas sembled SnO_2 NPs electrode (b) before and (c) after 50 cycles at 1 C, and (d) and (e) SEM images at high magnification of (b) and (c), respectively.

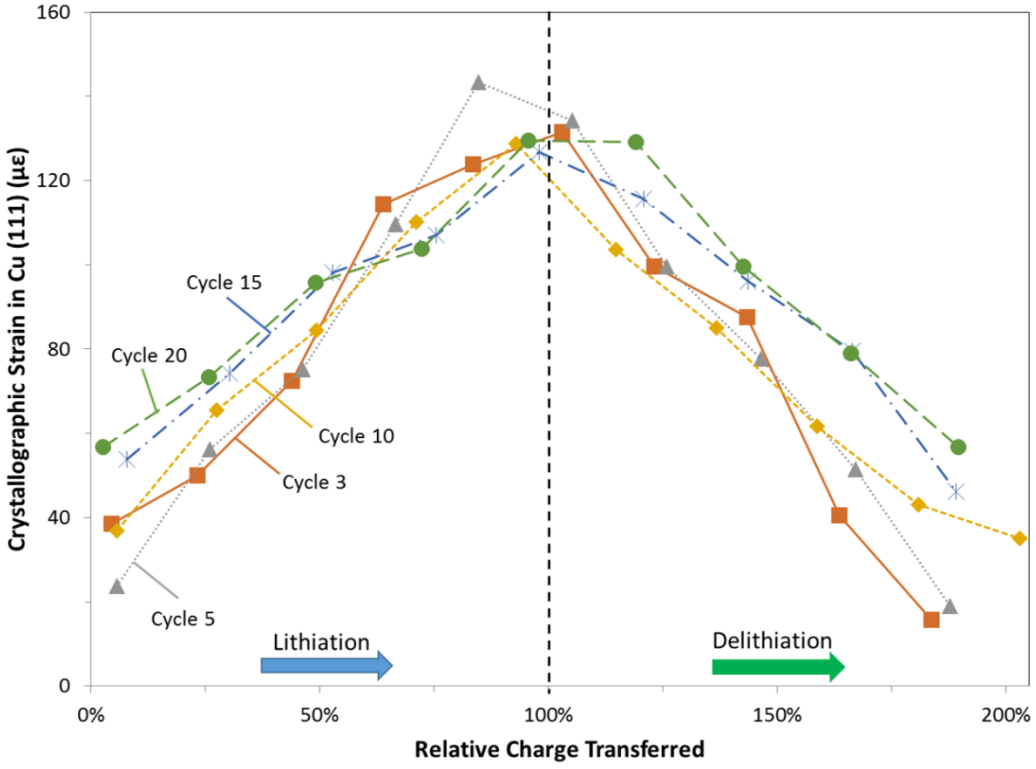

Fig. S8 A plot of average crystallographic strain in the Cu (111) diffraction ring versus the relative charge transferred during cycling, as measured by the fraction of the total amount of (de)lithiation charge transferred in each cycle when cycling the SnO_2/Cu foam@10M at 1C, as measured by in operando X-ray diffraction. The error in crystallographic strain calculation, based on the uncertainty in detector pixel fitting, is estimated to be smaller than the markers indicated for each cycle.

Table S1 Comparison of the electrochemical performance of Sn-based materials reported in literatures and this work.

	Voltage range / V	Cycle	Current density / mA g^{-1}	Capacity / mAh g^{-1}
Our data	0.01 - 2	50	781	621
Mesoporous TiO_2-Sn/C Core-Shell Nanowire Arrays[S3]	0.01 - 3	160	335	459
Three-Dimensional Porous Core-Shell Sn@Carbon Composite[15]	0.02 - 3	315	25	638
Tin-Core/Carbon-Sheath Coaxial Nanocables[33]	0.005 - 2.5	50	50	630
Graphene-Confined Sn Nanosheets[36]	0.005 - 2	60	50	590
3D Nanoporous Au-Supported Nanocrystalline Tin[S4]	0.005 - 2 0.005 - 1	140	100	420 599

Supplementary references

S1. N. Li, C. R. Martin and B. Scrosati, *Electrochem. Solid-State Lett.*, 2000, **3**, 316.

S2. N. Li and C. R. Martin, *J. Electrochem. Soc.*, 2001, **148**, A164.

S3. J.-Y. Liao and A. Manthiram, *Adv. Energy Mater.*, 2014, 1400403.

S4. Y. Yu, L. Gu, X. Lang, C. Zhu, T. Fujita , M. Chen and J. Maier, *Adv. Mater.*, 2011, **23**, 2443.

S5. Hammersley, *ESRF Intern. Rep.*, 1998, ESRF98HA01.

S6. A. P. Hammersley, S. O. Svensson, A. Thompson, H. Graafsma, A. Kvick, J. P. Moy, *Rev. Sci. Instrum.*, 1995, **66**, 2729.

S7. A. Wanner, D. C. Dunand, *Metall. Mater. Trans. A*, 2000, **31**, 2949.